Mixtures of Liquid-Crystalline and Amorphous Dicyanates: Unusual Curing Behavior and Mechanical Properties

Hilmar Körner, Atsushi Shiota, and Christopher K. Ober*

Department of Materials Science & Engineering, Cornell University, Bard Hall, Ithaca, New York 14853

Michele Laus

Dipartimento di Chimica Industriale e dei Materiali, Universita di Bologna, Viale Risorgimento 4, 40136 Bologna, Italy

Received December 17, 1996[⊗]

Three series of triazine networks were prepared by a thermal cyclotrimerization reaction between the mesogenic 1,4-benzenedicarboxylic acid bis(4-cyanatomethylphenyl) ester (LC1), 1,4-cyclohexanedicarboxylic acid bis(4-cyanatomethylphenyl) ester (LC2), and either one of two commercial nonmesogenic dicyanates, namely, the (1-methylethylidene)di-4,1-phenylene ester cyanic acid (B) and the [2,2,2-trifluoro-1-(trifluoromethyl)ethylidene]di-4,1-cyanic acid phenylene ester (F). The various mixtures display liquid-crystalline behavior provided that a minimum of 50% of the mesogenic dicyanates LC1 and LC2 are present. Isotropic or nematic networks can be obtained by appropriately adjusting the monomer composition. It can be shown that networks with reproducible properties could be prepared and studied for their thermal and dynamic-mechanical behavior only by additional curing at very high temperatures. The observed trend in temperature of the α relaxation in the investigated system with LC1 and LC2 is complex, and substantial deviations from linear behavior are observed. The data presented differ from previously reported liquid-crystal thermoset (LCT) systems and demonstrates that mixtures of LC and non-LC thermosets represent a delicate mesomorphic system. A thorough analysis was carried out, and the results will be discussed in detail.

Introduction

Liquid-crystalline thermosets combine high-dimensional stability and mechanical processability typical of polymer networks with the unique anisotropic behavior of liquid crystals.[1] In this respect, great attention is presently being directed to the synthesis of highly crosslinked networks[2,3] both as materials for nonlinear optics and electronic packaging and as matrix materials for advanced composites, among many other possible uses. For these highly demanding applications, it is essential to develop polymeric materials with optimized structures and precisely controlled architectures. There are three major types of LC thermosets. Bisacetylene-terminated rigid-rod monomers and the corresponding thermosets were studied by several groups.[4−6] Rigid-rod epoxy thermosets[7−10] are the broadest and most thoroughly explored thermoset system with more than 20 papers and patents published to date. Bismaleimide rigid-rod thermosets were studied earlier.[11] Research on structural LC thermosets has focused on mesophase-forming dicyanate esters which can cure into LC triazine networks.[12−16] In principle, these materials should combine the excellent thermal stability and dielectric properties that make cyanate ester thermosetting resins very attractive for circuit board fabrication[17] with the ability of liquid crystals to self-order into supramolecular structures capable of being macroscopically oriented by external electric[18] and magnetic fields.[12]

A very effective method of tailoring mesophase transitions and tuning physical properties to desired levels is by the copolymerization of mixed LC and non-LC

[⊗] Abstract published in *Advance ACS Abstracts,* June 1, 1997.

(1) Gleim, W.; Finkelmann, H. *Side Chain Liquid Crystal Polymers*; McArdle, C. B., Ed.; Blackie: Glasgow, 1989; p 287.
(2) Shiota, A.; Ober, C. K. *Prog. Polym. Sci.*, in press.
(3) Barclay, G. G.; Ober, C. K. *Prog. Polym. Sci.* **1993**, *18*, 899.
(4) Melissaris, A. P.; Litt, M. H. *Macromolecules* **1994**, *27*, 2675.
(5) Melissaris, A. P.; Sutter, J. K.; Litt, M. H.; Scheiman, D. A.; Scheiman, M. *Macromolecules* **1995**, *28*, 860.
(6) Douglas, E. P.; Langlois, D. A.; Benicewicz, B. C. *Chem. Mater.* **1994**, *6*, 1925.
(7) Barclay, G. G.; Ober, C. K.; Papathomas, K. I.; Wang, D. W. *J. Polym. Sci., Polym. Chem. Ed.* **1992**, *30*, 1831.
(8) Barclay, G. G.; McNamee, S. G.; Ober, C. K.; Papathomas, K. I.; Wang, D. W. *J. Polym. Sci., Polym. Chem. Ed.* **1992**, *30*, 1845.
(9) Carfagna, C.; Amendola, E.; Giamberini, M. *J. Mater. Sci. Lett.* **1994**, *13*, 126.
(10) Carfagna, C.; Amendola, E.; Giamberini, M.; Filippov, A. G. *Makromol. Chem. Phys.* **1994**, *195*, 279.
(11) Hoyt, A. E.; Benecewicz, B. C. *J. Polym. Sci., Polym. Chem. Ed.* **1990**, *28*, 3403.
(12) Barclay, G. G.; Ober, C. K.; Papathomas, K. I.; Wang, D. W. *Macromolecules* **1992**, *25*, 2947.
(13) Ou, J. C.; Hong, Y. L.; Yen, F. S.; Hong, J. L. *J. Polym. Sci., Polym. Chem. Ed.* **1995**, *33*, 313.
(14) Koerner, H.; Ober, C. K. *Polym. Mater. Sci. Eng. Prepr.* **1995**, *73*, 456.
(15) Mormann, W.; Zimmermann, J. *Macromol. Symp.* **1995**, *93*, 97.
(16) Wang, Y. H.; Hong, Y. L.; Yang, F. S.; Hong, J. L. *Polym. Mater. Sci. Eng. Prepr.* **1994**, *71*, 678.
(17) Papathomas, K. I.; Wang, D. W. *J. Appl. Polym. Sci.* **1992**, *44*, 1267.

S0897-4756(96)00642-4 CCC: $14.00

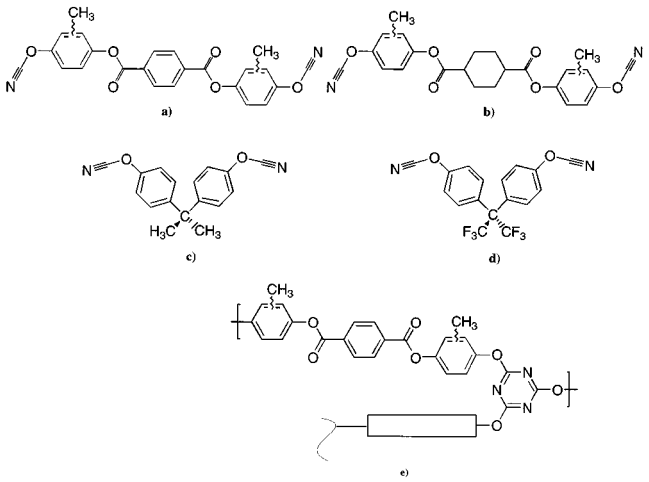

Figure 1. Chemical structures of studied compounds (a) LC1, (b) LC2, (c) B, (d) F, and (e) network structure of compound LC1.

monomers.[19−21] In fact, by appropriate adjustment of the overall composition it is possible to predetermine the precise mesophase behavior in statistical copolymers. The extension of this concept to the synthesis of networks containing at least one mesogenic component is highly promising since LC thermosets with very unusual properties may be obtained without the constant redesign of the macromolecular structure. Blending of thermosetting monomers enables us to improve molecular packing factors, and by choosing compounds with the right molecular architecture, unusual mechanical and thermal properties can be induced. However, this possibility has not yet been systematically explored and will be demonstrated in this work.

Our goal was to apply the concept of mixtures to the preparation of several dicyanate compositions, produced by adding either the mesogenic dicyanates of bis(4-hydroxymethylphenyl) terephthalate (LC1) or 4-cyclohexanedicarboxylic acid bis(4-cyanatomethylphenyl) (LC2) ester (structures shown in Figure 1) to either one of the two commercial monomers, namely, the (1-methylethylidene)di-4,1-phenylene ester cyanic acid (B) and the [2,2,2-trifluoro-1-(trifluoromethyl)ethylidene]di-4,1-cyanic acid phenylene ester (F).

The necessary conditions for obtaining networks with reproducible characteristics will be given in this paper, and their liquid-crystalline and dynamic-mechanical properties described in detail. It will be shown that networks with unusual thermal and dynamic-mechanical behavior are obtained. The mesogenic potential of compounds LC1 and LC2 enables us to produce liquid-crystalline mixtures even with more than 50% of non-LC thermosetting monomers. These new materials with tunable optical and mechanical properties are promising candidates for a variety of applications where conventional thermosets are being used and can be easily prepared by mixing in LC compounds such as LC1 or LC2.

(18) Körner, H.; Shiota, A.; Ober, C. K.; Bunning, T. *Science* **1996**, *272*, 252.
(19) Engel, M.; Hisgen, B.; Keller, R.; Kreuder, W.; Reck, B.; Ringsdorf, H.; Schmidt, H. W.; Tschirner, P. *Pure Appl. Chem*. **1985**, *57*, 1009.
(20) Percec, V.; Lee, M. *J. Mater. Chem*. **1991**, *1*, 1007.
(21) Laus, M.; Bignozzi, M. C.; Angeloni, A. S.; Galli, G.; Chiellini, E. *Macromolecules* **1993**, *26*, 3999.

Table 1. Values of the α-Relaxation Temperature[a] of Networks and Pure Monomers

sample	content of LC1/wt %	Tα/°C	sample	content of LC1/wt %	Tα/°C
N−LC1	100	215			
N−LC1/B20	80	247	N−LC1/F20	80	260
N−LC1/B40	60	272	N−LC1/F40	60	276
N−LC1/B60	40	274	N−LC1/F60	40	287
N−LC1/B80	20	272	N−LC1/F80	20	290
N−B	0	279	N−F	0	258[b] (288)

[a] Estimated as corresponding to the maxima of the tan δ peaks in the dynamic-mechanical curves. [b] Corrected by DSC experiments of a sample postcured at 350 °C resulting in the value in parentheses.

Experimental Section

Materials. The (1-methylethylidene)di-4,1-phenylene ester cyanic acid (B) and [2,2,2-trifluoro-1-(trifluoromethyl)ethylidene]di-4,1-cyanic acid phenylene ester (F) were kindly provided by IBM Systems Technology Division and used without further purification. The dicyanate of 1,4-benzenedicarboxylic acid bis(4-cyanatomethylphenyl) ester (LC1) was synthesized, as described elsewhere,[12] by reacting the terephthaloyl chloride with a large excess of methylhydroquinone. The bisphenol so obtained was then treated, without any purification, with cyanogen bromide, in the presence of triethylamine, to give dicyanate LC1. A modified procedure was employed consisting of the use of a 5:1 excess of cyanogen bromide instead of the 2:1 excess used in previous work.[7] In this case, the precipitation of LC1 from chloroform solutions into hexane yields pure dicyanate with approximately 85% of the theoretical yield. The liquid-crystalline compound LC2 was synthesized in the same way.

Triazine Networks N−LC1, N−B, N−F, N*−LC1/B20−80, and N−LC1/F20−80.* The triazine networks N−LC1, N−LC2, N−B, and N−F were prepared by thermal cyclotrimerization of the dicyanates LC1, LC2, B, and F, respectively. In particular, the networks are designated with the acronym N−LC1/B*m* and N−LC1 or LC2/F*m*, where *m* represents the weight percentage of monomer B or F in the reaction mixture. Networks N−LC1/B20−80, N−LC1/F20−80, and N−LC2/F20−80 were obtained by mixing suitable proportions of LC1 and LC2 with monomers B or F. Table 1 reports the various mixture compositions. The mixtures were prepared by dissolving the appropriate amounts of LC1 or LC2 and B or F in chloroform. Furthermore, the solvent was evaporated, and the mixtures were dried in a vacuum oven at room temperature. The cyclotrimerization reactions were performed by heating the dicyanate LC1 or LC2, B and F, as well as the mixtures of monomers LC1 or LC2 and B or LC1 and F to 190 °C, maintained at this temperature for 30 min, and then heated to 230 °C for 3 h. Finally, a postcuring step consisting of a further heating of the samples to 270 °C for 30 min was adopted. Microscopy and DSC observations were performed on the dicyanates LC1 or LC2 and on the mixtures placed on glass plates or into aluminum pans and heated to the cyclotrimerization temperature. Dynamic-mechanical measurements were performed on rectangular sheets prepared by introducing the powdered LC1, B, and F samples as well as various combinations thereof into a rectangular mold. The entire assembly was placed between press plates with a nominal pressure of 5 tons cm^{-2} and let stand at room temperature. After 20 min, the sample sheet was inserted between two KBr plates, placed again between the press plates with a nominal pressure of 5 tons cm^{-2} and maintained at this pressure for 10 min. The temperature was then raised to 190 °C, the pressure released to 0.5 tons cm^{-2} and the curing let to proceed for 30 min and then heated to 230 °C for 3 h. Finally, a postcuring step consisting of a further heating of the samples to 270 °C for 30 min was adopted. It could be shown that for some mixtures another step at temperatures higher than 300 °C was necessary to get reproducible data. The networks were recovered as rectangular 18 × 5 × 1 mm sheets by dissolving the KBr windows in water.

Physicochemical Characterizations. Curing reactions and phase transitions were studied by differential scanning calorimetry and polarizing optical microscopy (DSC and POM). The analyses were carried out under dry nitrogen flow with a TA Instrument DSC 910. Optical microscopy observations were performed on polymer films on glass slides with a Nikon Optiphot2-POL optical polarizing microscope (POM) equipped with a Mettler FP-82 hot stage. Mesophases were examined at a magnification of 100× and 200×. To obtain numerical information about the growth of the liquid-crystalline state, the POM was equipped with a Mettler 17517 photomonitor. Light intensity, caused by birefringence of the samples, was recorded by a personal computer system.

Time-resolved FT/IR spectra were carried out either by melt-pressing the samples or by casting films from a solution of the samples in $CHCl_3$ onto sodium chloride windows. The NaCl plates were placed in a hot stage, which was then mounted inside a Mattson 2020 Galaxy Series FT/IR spectrometer. Scans at 0.7−0.9 min intervals were chosen, and the temperature of the hot stage set to the curing temperatures. The curing reaction was monitored following the decrease of the absorption intensity at 2268 cm^{-1} (CN stretching) and the corresponding increase of the absorption intensities at 1564 and 1370 cm^{-1} (aromatic CN stretching). Problems of baseline and changes in the film thickness were corrected by inner standards (absorbances at 2000 and 1014 cm^{-1}, respectively). Dynamic-mechanical measurements were performed with a dynamic-mechanical analyzer (Perkin Elmer DMA-7, at a scanning rate of 4 °C min^{-1} and 1 Hz frequency) using the three-point bending geometry.

Results and Discussion

Synthesis of Networks. Networks N−LC1 or LC2, N−B, and N−F were prepared by thermal cyclotrimerization of the dicyanates LC1, LC2, B, and F, respectively. Networks N−LC1/B N−LC1/F or LC2/F were prepared by thermal cyclotrimerization of mixtures of monomers LC1 and B or LC1 or LC2 and F at different compositions. Samples were thermally cured for a selected time (45 min for LC1 mixtures and 2.5 min for LC2 mixtures) at the target temperature. To find the best conditions for the cyclotrimerization reaction, FT/IR and DSC studies were performed.

FT/IR Measurements. As the trimerization reaction proceeds, the nitrile bonds of the dicyanates are converted into aromatic C═N bonds building up triazine rings. Due to the isolated CN absorbance, the kinetics of the cyclotrimerization reaction can be monitored by time-resolved FT/IR. For samples with more than 50% of monomer LC1 or LC2, birefringence occurs after curing for several minutes, indicating a phase transition. This effect may provide an additional contribution to transmittance of IR through the sample. We were unable to observe a sudden increase in the baseline of the absorbance as observed in a similar system by Mormann et al.[15] In addition, it is known that significant change in the refractive index increment from the monomer to the thermoset was found to make a precise determination of the monomer/thermoset ratio from FT/IR data difficult.[22] The curing reaction was assumed complete when the absorption intensity at 2268 cm^{-1} disappeared. Figure 2 shows the 2000−2500 cm^{-1} FT-IR spectral region of monomer LC1 cured at 230 °C.

Let α be the conversion of the dicyanate function, then $d\alpha/dt$ displays the change of the curing rate of the system. The conversion can be directly calculated from the absorbance, when the absorbance for the fully cured

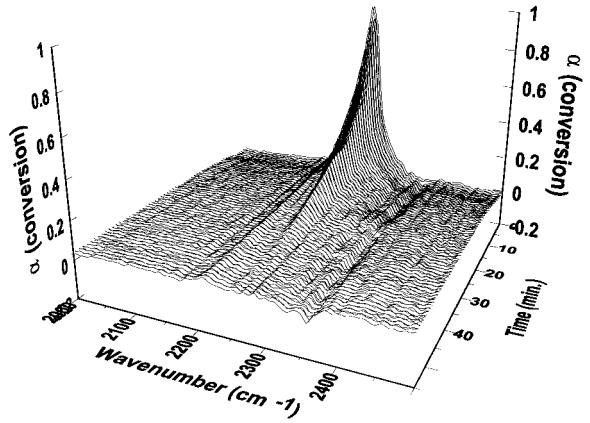

Figure 2. FT/IR spectra in the 2000−2500 cm^{-1} region versus time for monomer LC1 cured at 230 °C.

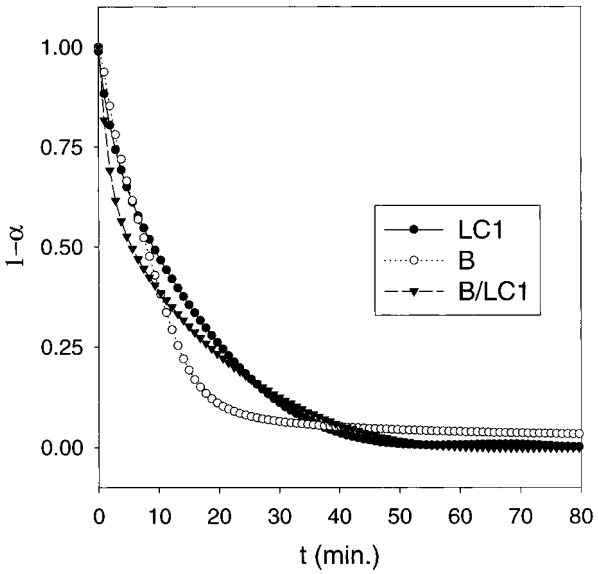

Figure 3. Change of the nitrile absorbance at 2268 cm^{-1} for monomer LC1 and an equimolar mixture of LC1 with B cured at 230 °C.

thermoset and the monomer before curing is known. In this respect Figure 3 displays the conversion and the decrease of the nitrile absorbance at 2268 cm^{-1} with time at a temperature of 230 °C. The same figure also shows the results for B and equimolar mixtures of LC1 with B, cured at 230 °C. A comparison between the samples B, LC1, and their equimolar mixture at 230 °C shows that there are differences present in the curing of these compounds. In particular, the curing of compound B shows initially a slower curing rate, but the kinetics do not change between a maximum at 6−25 min (constant slope, Figure 4). For the mixtures, on the other hand, the kinetics change soon after 5 min (a more asymmetrical $d\alpha/dt$ curve in Figure 4b which tapers off more gradually) and ultimately the pure B cures faster than the mixtures at a curing temperature of 230 °C.

Figure 4 shows two different regions over the curing reaction, fast curing in the first 20 min, and slower curing after 20 min which indicates diffusion control in this later stage of the polymerization reaction. In some cases the onset of gelation could be seen by FT/IR as a plateau in the absorbance at 1566 and 1362 cm^{-1}. The changes in the slope of the absorbance/time curves occur at a conversion between 50% and 60%. Although this

(22) Bauer, M.; Bauer, J.; Kuehn, G. *Acta Polym.* **1986**, *37*, 715.

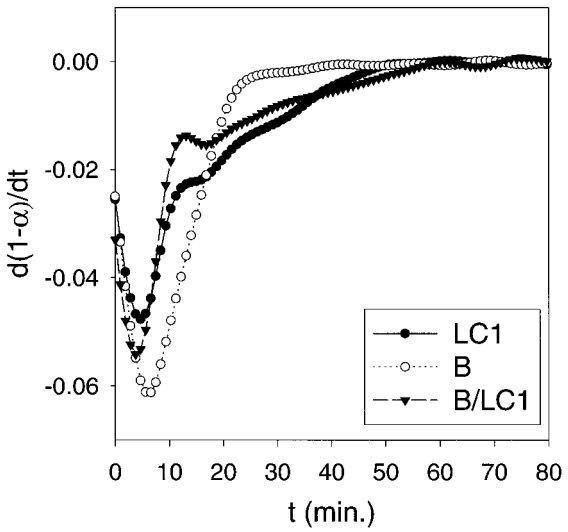

Figure 4. Calculated first derivatives of the absorbance for monomer LC1 and equimolar mixture of LC1 with B cured at 230 °C.

experiment shows such behavior at several different temperatures, scattering of the data makes it impossible to get a reliable value of conversion at the gelation point. We would like to point out the discrepancy found in the literature where a variety of values for conversion at gelation are found and differ from theoretical values for dicyanate thermosets.[23,24]

Thermal Analysis by DSC of Partially Cured Samples. To complete the studies of the curing process, a thorough thermal analysis was performed on both the dicyanates and the relevant mixtures. The samples were heated to a predetermined curing temperature *T*(cure) between 140 and 270 °C, held at the curing temperature for 45 min, and then cooled to room temperature. Figure 5 illustrates the DSC heating curves of monomer LC1 after the above-mentioned procedure at various temperatures. This monomer displays a more complex thermal behavior than the non-LC monomers and their mixtures, involving a series of broad endothermic and exothermic transitions. There are several distinct reasons for this behavior: Monomer LC1 is a mixture of three isomers that differ in the relative position of the methyl groups, and consequently broad DSC melting curves can be expected. In addition, the exothermic transition due to the cyclotrimerization reaction can be partially superimposed with a small endothermic transition due to the clearing of the formed liquid-crystalline phase. For monomers B and F the DSC curves are significantly narrower due to the purity of these compounds (no isomers present). For all compounds, curing enthalpies of about 100 kJ/mol are found, which are in good agreement with reported experimental values of other dicyanates.[23] DSC traces of some mixtures are shown in Figure 8 and discussed later.

Figures 6 and 7 display the extent of curing (α), as determined from the ratio between the enthalpy of the DSC peaks of samples after curing at the given temperature, and the total cyclotrimerization enthalpy,

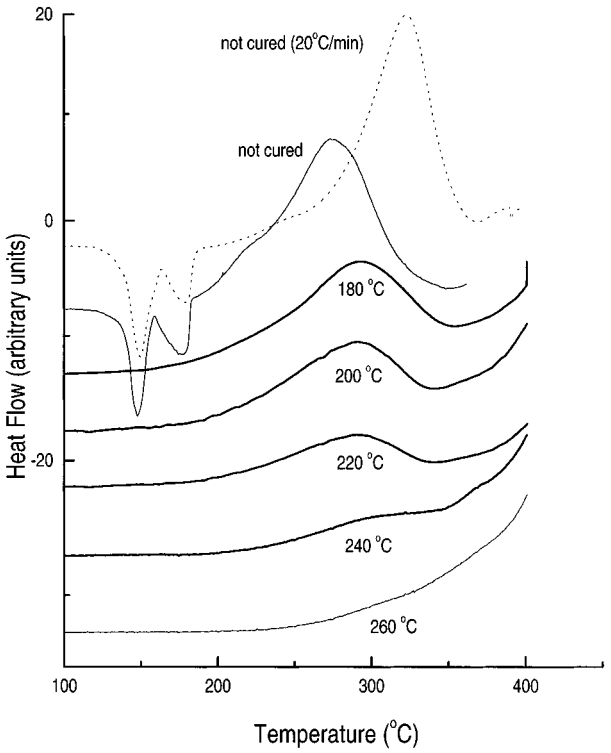

Figure 5. DSC heating curves of monomer LC1 following curing at various temperatures T_{cure}.

evaluated from untreated samples, as a function of the curing temperature for monomers and all mixtures. For mixtures LC1/F a curing temperature of 270 °C leads to practically quantitative conversion as shown in Figure 6a. Figure 6b shows the results for series LC1/B and Figure 6c for the mixtures LC2/B. In Figure 7, on the other hand, the composition of the mixtures is plotted versus the extent of curing for all mixtures under study. It can be seen that the curing behavior of these mixtures is very complex and does not follow linear behavior as one might expect from homogeneous mixtures. Figure 7b displays the extent of polymerization versus the composition of the mixtures. Nonlinear behavior can be seen for the system with the low-reactivity, high-T_g monomer B and the highly reactive, low-T_g monomer LC1. The activation energy for the curing reaction of LC1 is at 67.5 kJ/mol,[25] lower than for compound B with a reported value of 80−96 kJ/mol. The T_g of a fully cured network of LC1 is 222 °C, while that of B is 280 °C.

The unusual results from the temperature scans in DSC experiments, summarized in Figures 6 and 7, may be interpreted as a synergistic effect. As explained previously, curing below T_g of the network leads to diffusion control after a specific extent of polymerization. In this diffusion-controlled region, the free volume of the system dominates the reaction kinetics. The free volume is mainly determined by the packing of the compounds upon network formation, which is a function of both the molecular shape and size of the present molecules. LC1 possesses a rigid-rod and linear molecular shape and produces a relatively larger free volume which may be due to the presence of the methyl groups

(23) Bauer, M.; Bauer, J. *Chemistry and Technology of Cyanate Ester Resins*; Hammerton, I., Ed.; Chapman and Hall: New York, 1994; p 61.

(24) Gupta, A. M.; Macosko, C. W. *Macromolecules* **1993**, *26*, 2455.

(25) Shiota, A.; Koerner, H.; Ober, C. K. Liquid Crystalline networks from 1,4-Benzenedicarboxylic acid bis(4-cyanatomethylphenyl) ester. Submitted to *Macromol. Chem. Phys.*

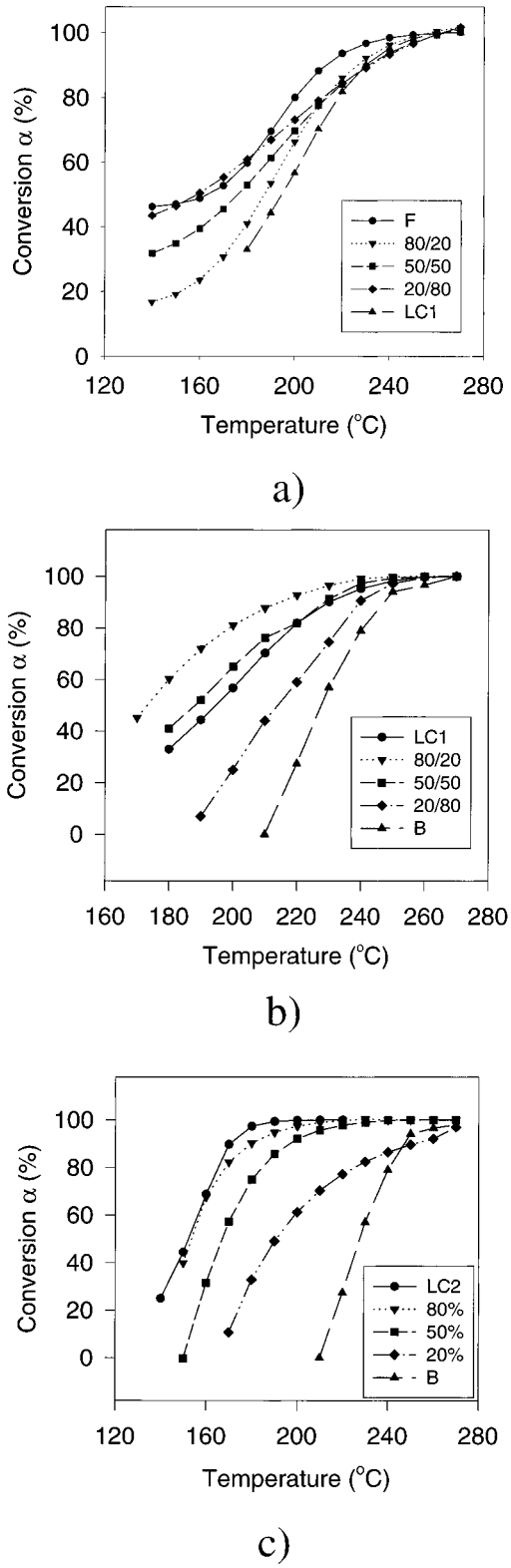

Figure 6. Cyanate conversion as a function of curing temperature for mixtures (a) LC1/F, (b) LC1/B, and (c) LC2/B derived from DSC data.

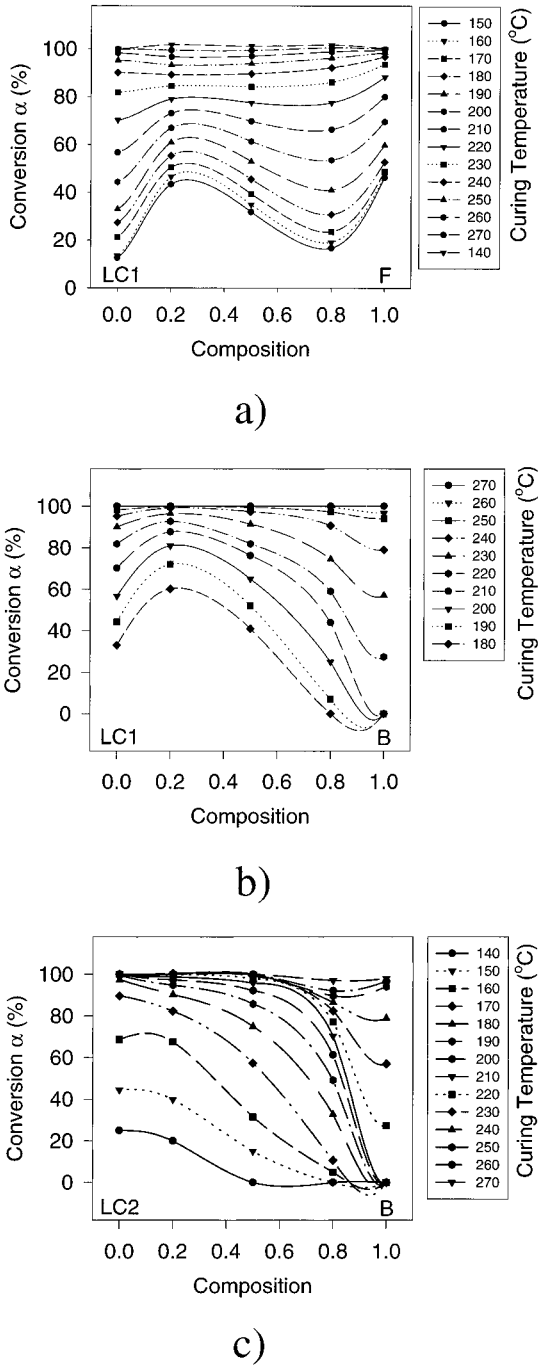

Figure 7. Cyanate conversion as a function of composition for all mixtures: (a) mixtures LC1/B; (b) mixtures LC1/F; (c) mixtures LC2/B.

attached to the phenyl rings or repulsion between the linear shaped molecules (LC-field) and cross-link sites, compared to compound B. Compound B, in addition, has the two cyanatophenyl groups connected via an isopropylidene linking group which allows production of a lower free volume and the resulting high T_g in the final network. Increasing the amount of LC1 up to 80% in a sample with B resulted in a faster reaction as well as a higher extent of polymerization. This higher extent of curing can be attributed to an increase of mobility in the diffusion-controlled region. In addition, an activated reaction intermediate may also compensate for the reactivity of monomer B. This cooperative effect in a mixture of two very different compounds results in a maximum in the extent of polymerization at a composition of B/LC1 = 20/80. The presence of small amounts of B, which has a bent molecular shape, in a sample of the linear shaped LC1 may allow a more efficient molecular packing in the network than in the pure LC1 network system.

Compound LC2 also has a higher reactivity and a lower T_g when cured than monomer B. However, due to the presence of the more flexible cyclohexane ring in

the core of the molecule, a similar synergism as seen in the mixture B/LC1 = 20/80 was not observed. In this case the dependence of the extent of the polymerization reaction on the composition of the system shows an almost linear behavior, compared to mixtures of B and LC1.

In contrast to a combination of B/LC1, as shown in Figure 7a, a mixture of F/LC1 shows more complicated behavior. In this case, monomer F has a higher reactivity, and when cured a higher T_g than compound LC1. A high rate constant frequency factor, mainly due to low viscosity in monomer F, contributes to the high reactivity, even though molecular orbital calculations for both monomers B and F show almost identical electron density distributions and identical potentials for the HOMO and LUMO orbital. We assume that existence of small amounts of up to 20% LC1 in monomer F reduces the reaction rate in the curing system, due to an increase of the viscosity. However, an increase of free volume as well as better molecular packing causes an improved conversion in the composition range between F/LC1 = 80/20 and 20/80, as shown in Figure 7b.

In short, the complex trend in the extent of curing versus composition is mainly controlled by synergism of several factors such as packing coefficient, reactivity, T_g, and collision factor (viscosity). X-ray studies of networks LC1 and LC2 demonstrate that the stiff architecture of LC1 leads to an unusually high value of the wide-angle reflection (5.3 Å), even in the liquid-crystalline state and the final LC network. Although compound LC2 also has methyl groups attached to phenyl rings, the flexible cyclohexane ring can adjust to steric incompatibilities and curing results in much better packing with a wide-angle reflection of 4.7 Å.

Another significant difference between mixtures of F and B is observed by DSC. Two broad, distinct maxima for the curing process are detected for the series of mixtures with compound F but only one curing exotherm can be observed for the B/LC1 series (Figure 8). The difference in behavior could be due to phase separation, but POM observations show that no evidence of phase separation is present which would be apparent by LC droplets in an isotropic matrix of F. An interpretation based on different reactivity of the non-liquid-crystalline compounds B and F cannot be made according to molecular calculations. Further experiment on the LC nature of the mixtures is necessary and will be subject of a forthcoming publication.

Curing conditions were optimized with combined DSC and FT/IR data as follows: the samples were heated to 190 °C, maintained at this temperature for 30 min, and then heated to 230 °C for 3 h. Finally, a postcuring step consisting of further heating of the samples to 270 °C for 30 min was employed. The above thermal treatment was found to be optimal for achieving networks of monomer B with reproducible thermal and mechanical transitions and materials without any thermal degradation. For mixtures with F, a shorter curing cycle at temperatures higher than 300 °C is necessary to complete network formation, although FTIR shows complete conversion of cyanate groups.

Liquid-Crystalline Behavior by Polarizing Optical Microscopy. The nature of the liquid-crystalline phases of the various mixtures was investigated by observations of optical textures in a hot stage of a polarizing microscope. The various samples were placed into the hot stage and heated to selected temperatures, and the evolution of the optical textures was observed between crossed polarizers. The phase behavior of compound LC1 is already known from previous work.[12,25] When heating above 160 °C, the sample melts into an isotropic phase, and after 5−30 min, depending on the curing temperature, a nematic phase evolves. After an induction time (5−30 min) droplets increase in size and number and build a homogeneous marbled nematic (with cover glass) or a nematic Schlieren texture (without cover glass).

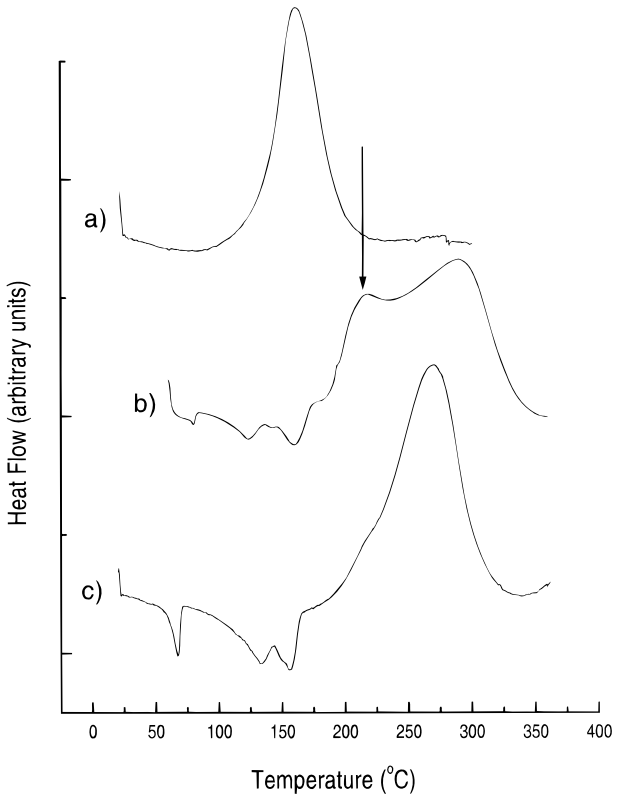

Figure 8. DSC traces of 1/1 mixtures (by weight) of (a) LC2/B, (b) LC1/F, and (c) LC1/B. Two distinct maxima can be observed for LC1/F (arrow denotes first maximum).

The process of LC formation is fast, and the entire sample shows a nematic texture within minutes after appearance of LC droplets. Depending on the treatment of glass slides, a Schlieren texture also formed as shown in Figure 9 for mixtures LC1/B10 and LC1/B50. After complete curing, a disclination-rich nematic Schlieren texture was observed. The thermosetting monomer LC2 melts into a nematic phase at a temperature of 155 °C. Mixtures of LC1 or LC2 with B or F display liquid-crystalline behavior provided that a minimum of 25% of LC1 or LC2 is present. In compositions containing less than 25% of LC1 or LC2, the cured networks of mixtures are isotropic. To achieve a more quantitative analysis of birefringence development, a photomonitor was used to record changes while the compound was cured. The guest/host nature of the liquid-crystalline phase at high ratios of the non-LC compounds will be studied in more detail and published in a forthcoming paper.

The results from POM experiments for compound LC1 and mixtures with compound B at different curing temperatures are shown in Figure 10. The compound starts to cure in the isotropic phase and no change in

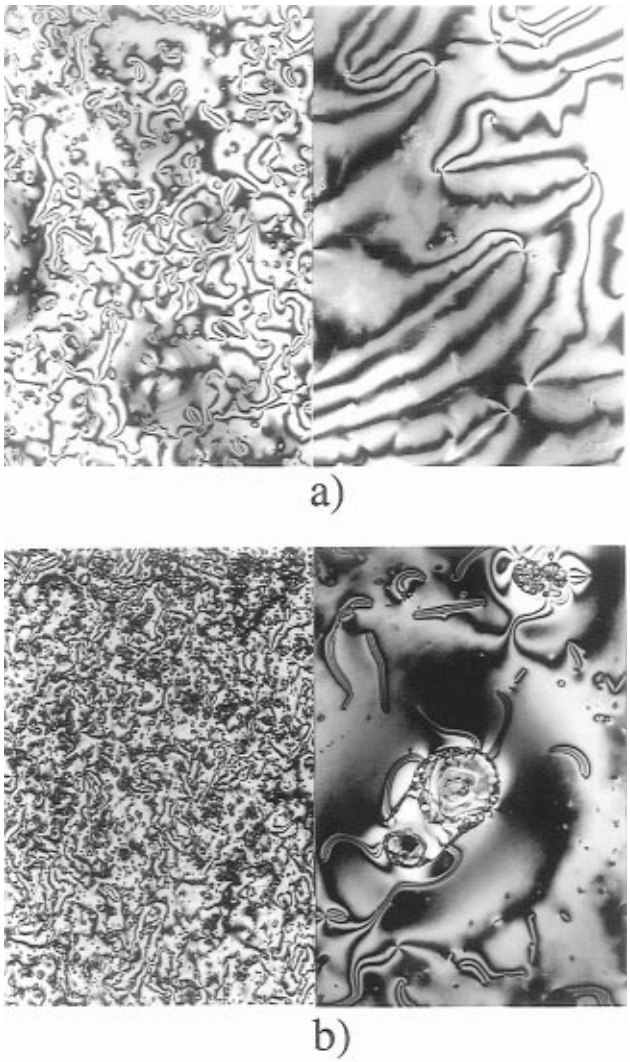

Figure 9. Optical photographs of mixtures LC1/B cured at 200 °C: (a) 10% B; (b) 50% B. Right side shows enlargement.

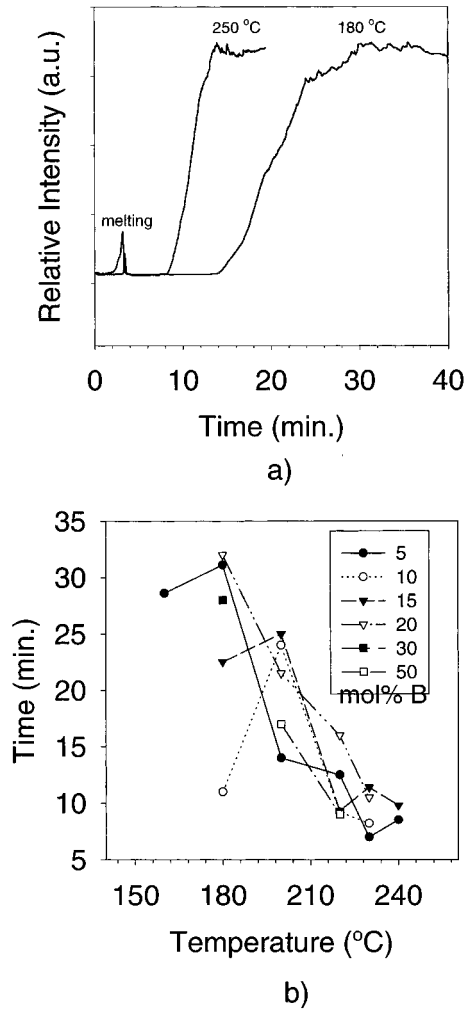

Figure 10. (a) Occurrence of the LC phase seen in the increase of birefringence for mixture LC1/B5 cured at 180 and 250 °C; (b) time/temperature graph derived from birefringence data by POM for mixtures LC1/B.

birefringence is seen. After an induction time of several minutes a sudden increase of birefringence is detected, which first shows an exponential growth in birefringence, followed by a plateau. The compound tends to align homeotropically between the glass substrates leading to a decrease in birefringence. This effect is very important for the interpretation of this system. Mixtures prepared between glass slides and cover glasses show no birefringence already at compositions of less than 25% B, indicating a homeotropic alignment, as will be explained in the following. Without the cover glass a nematic Schlieren texture is observed in mixtures of more than 50% B. According to these observations it is possible to obtain isotropic or nematic networks by an appropriate adjustment of the monomer composition and the curing temperature. Figure 10b shows the time/temperature behavior of mixtures with up to 50% of compound B in mixtures LC1/B. The time of the occurrence of the LC phase was derived from the onset of the increase of birefringence in Figure 10a. Decreasing the temperature leads to longer induction times as should be expected. Increasing the amount of B results in the same effect but less pronounced. At low temperatures the system behaves in a very complex manner which we cannot explain at this point.

Dynamic-Mechanical Behavior. The dynamic-mechanical behavior of networks N−LC1, N−B, N−F, N−LC1/B, and N−LC1/F was studied in the linear viscoelastic range at 1 Hz frequency over a wide temperature range from −120 to 300 °C. The transition temperatures of the dynamic-mechanical processes, estimated as corresponding to the maxima of the relevant tan δ peaks, are collected in Table 1.

Figure 11 illustrates the trends of the loss tangent (tan δ) as well as of the storage (G') and loss (G'') components of the flexural modulus as a function of temperature for sample N−B, as a typical example. G' decreases as temperature increases, with definite drops in G', corresponding to the main relaxation regions.

In particular, a slightly pronounced decrease of G' at about 7 °C, due to the β relaxation, preceded a significant drop of G' of 2 orders of magnitude at about 267 °C associated with the α relaxation of the network. In addition, well-defined maxima in the G'' and tan δ curves are observed in correspondence to the β and α relaxation processes.

Figures 12 and 13 show trends of the dynamic G' and tan δ for networks N−LC1, N−B, and N−LC1/B and for networks N−LC1, N−F, and N−LC1/F, respectively. G' of all the samples was approximately 3 GPa at −120 °C and decreased steadily with increasing temperature. In all samples, a drop in G' and a corresponding shallow peak in the tan δ curves was observed in the temper-

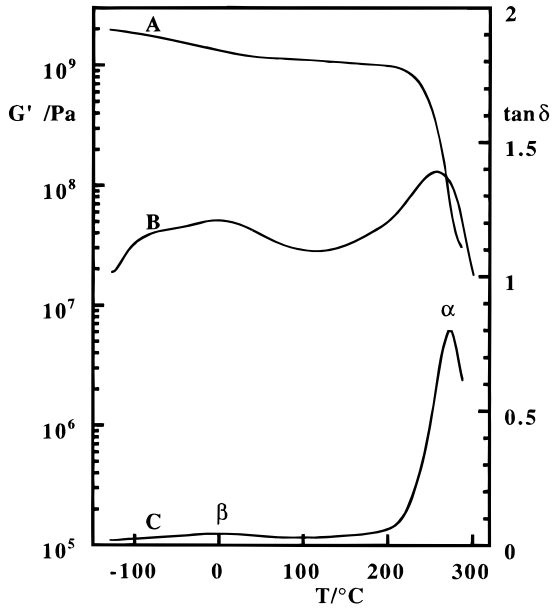

Figure 11. Change of the dynamic storage modulus (G', *A*) loss modulus (G'', *B*), and loss tangent (tan δ, *C*) versus temperature at 1 Hz for the network N−B.

ature range between 0 and 50 °C. This β relaxation was associated primarily with local mode processes of relatively short chain segments as, for example, phenyl ring reorientational motions. The β relaxation process in the cyanate mixtures is structured in at least two strongly overlapping components. Comparison of the β relaxation processes of the various networks, shown in the bottom of Figure 12, clearly indicates that the nature of the β-relaxation process of the mixtures is a result of the superposition of the individual β-relaxation processes of the networks.

The α-network relaxation is observed for all samples as a drop in G' in the temperature range between 200 and 300 °C. The breadth of the transition and the final value of the modulus are strongly dependent on the LC phase, and hence the composition of the mixtures. Comparing the trends of the tan δ curves in the α-relaxation region, it is interesting to note that in both systems the relaxation strength increases as the LC1 monomer content decreases. In addition, the width of the α-relaxation peak decreases as the LC1 monomer content decreases. This finding is different from the trend generally observed in binary mixtures where the width of the tan δ peak of the α-network relaxation, as a function of composition, passes through a maximum value. The low tan δ of the N−LC1 network can be ascribed to a rigid ordered structure which produces a high modulus in the rubbery region. The effect observed in the present systems could depend on the fact that monomer LC1 is a mixture of three isomers with different positions of the methyl groups. It should be pointed out that all mixtures display only one network relaxation peak, thus indicating that either the mixture is homogeneous or the size of the domains differing in composition in the phase-separated system is less than about 10 nm.[26]

The trend of the α network relaxation temperature, taken from the maximum in the tan δ peaks of networks

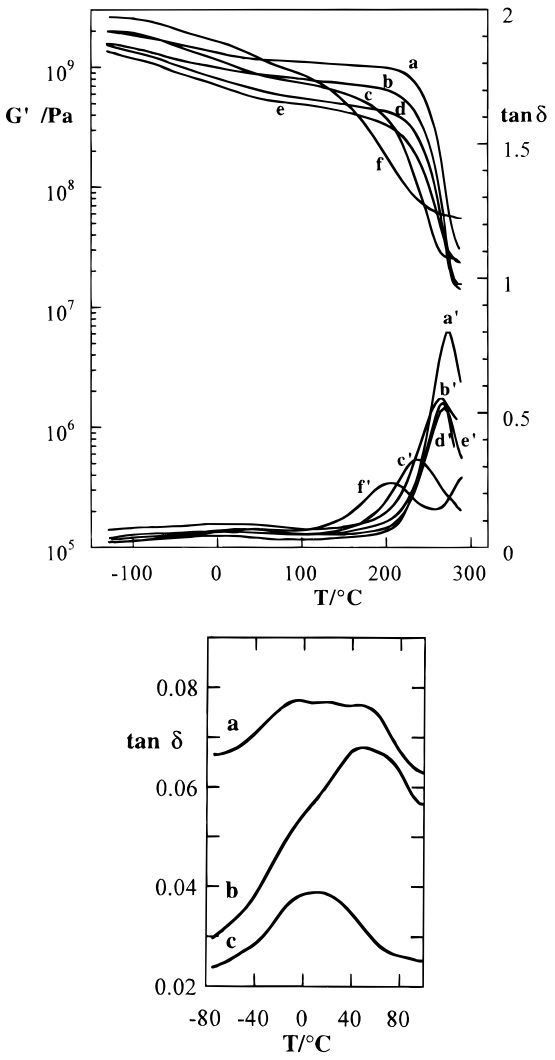

Figure 12. Top: loss tangent (tan δ) and the dynamic storage modulus (G') at 1 Hz versus temperature for thermosets LC1/B: (a) B; (b) LC1/B20; (c) LC1/B40; (d) LC1/B60; (e) LC1/B80; (f) LC1. Bottom: tan δ curves in the β-relaxation region of networks: (a) B; (b) LC1/B80; (c) LC1/B60 in an expanded scale.

N−LC1, N−B, N−LC1/B and networks N−LC1, N−F, N−LC1/F as a function of monomer LC1 content and networks N−LC2/B as a function of monomer LC2 content, is illustrated in Figure 14. The α-network relaxation temperature trend in the two systems with monomer LC1 is different. From DSC and FT/IR measurements the glass transition for pure monomer F can be explained by an incomplete curing reaction. Taking this into account, the glass transition of F cured to completion is much higher than shown by DMA measurements. Further DSC studies show the glass transition of a fully cured F sample to be 287 °C. With this corrected value for the glass transition both systems behave very similarly from DMA measurements. For samples N−LC1, N−B, and N−LC1/B, the α-network relaxation temperature is constant until the monomer LC1 concentration is lower than 60% and then decreases. With the corrected glass transition for samples N−LC1, N−F, and N−LC1/F these mixtures exhibit a similar trend but with higher glass transitions.

The substantial deviations of the α relaxation of both the network systems from linear behavior, often observed in binary systems,[26] could be indicative of the

(26) Utracki, L. A. *Polymer Alloys and Blends*; Carl Hanser Verlag: Munich, 1989; p 93.

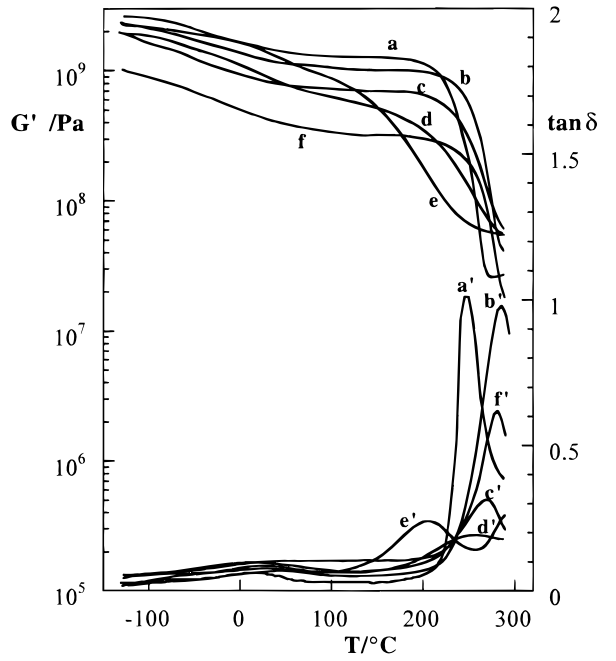

Figure 13. Loss tangent (tan δ) and the dynamic storage modulus (G') at 1 Hz versus temperature for thermosets N−LC1/F: (a) F; (b) LC1/F20; (c) LC1/F40; (d) LC1/F60; (e) LC1; (f) LC1/F80.

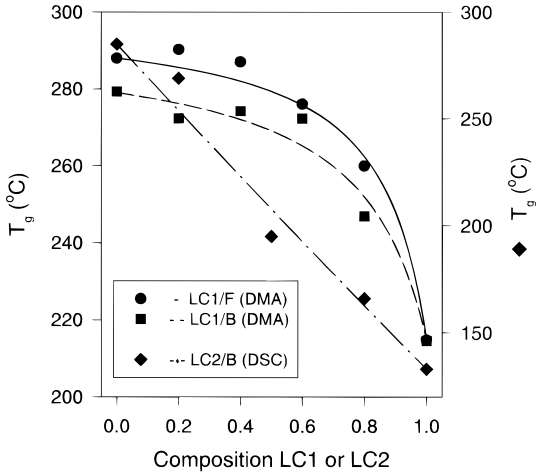

Figure 14. Glass transition temperatures for thermosets B/LC1, F/LC1, and B/LC2 as a function of monomer LC1 or LC2 content together with fit curves obtained using eq 1 (K = 5.42 for LC1/B, K = 7.42 for LC1/F, K = 0.96 for LC2/B).

presence of specific interactions between the different dicyanate monomers (LC1 and non-LC). These intermolecular interactions may produce a reduction of the free volume and consequently an increase in the α-relaxation temperature value with respect to the value expected for a noninteracting system. This explanation is in good agreement with the findings for the extent of polymerization in the mixtures from DSC results shown in the previous section. In addition, the different reactivity of B compared to LC1 could generate an intrinsic inhomogeneity within the networks and could cause the formation of clusters consisting of the more reactive monomer, thus making these networks multiphase systems. On the other hand, it was shown by POM observations that no phase separation was seen at least by the presence of LC droplets in any of the mixtures. In this case, the size of the domains, built up by phase separation, is important, and other microscopic measurements have to be taken to study this finding in more detail (SEM or TEM). SEM results, currently done on fractured samples, however, do not show any indication to support this assumption.

In this regard, the α-network relaxation temperatures as a function of the LC1 monomer composition can be best fitted by applying the Gordon−Taylor equation (eq 1), which has the following form:[27]

$$w_1(T_{g1} - T_g) + Kw_2(T_{g2} - T_g) = 0 \qquad (1)$$

In this equation, w_1 and w_2 represent the weight fraction of generic components 1 and 2, and K is an empirical parameter that measures the miscibility and the interaction between the two components. Although this equation is typically used to describe the glass transition temperature as a function of composition in multiphase systems such as miscible or immiscible blends,[28] it seems appropriate to try to extend its use to these peculiar network systems. The best-fit curves are reported as lines in Figure 14. Comparing the experimental data with the data fit, it appears that the α-network relaxation trend of the system consisting of samples N−LC1, N−B, and N−LC1/B is best described by the Gordon−Taylor equation with K = 5.45, whereas the α-network relaxation trend of the system consisting of samples N−LC1, N−F, and N−LC1/F results in a value of K = 7.43. For the network system N−LC2/B glass transition temperatures were obtained by DSC measurements and a fit shows an almost linear behavior in Figure 14 with a value of K = 0.96. Attempts to fit the data according to Simha[29] resulted in a much poorer fit.

The morphology of fractured samples of the above networks is currently being tested by SEM. The apparent differences between samples revealed by SEM and additional POM experiments will be presented in an upcoming publication.

Curing in the LC phase is very different than curing in the isotropic phase. Especially at higher conversions and higher temperatures the diffusion in a liquid-crystalline phase must be different from an isotropic one due to the one-dimensional order of the nematic phase. The possibility of formation of dimers which leads to extended linear chain growth at the beginning of the curing reaction as proposed in refs 30 and 31 might be enhanced in a nematic phase. The tan δ curves of the pure LC networks show an additional relaxation at about 300 °C, which is due to a postcuring effect or the appearance of a side reaction. DSC studies also show that samples cured under these conditions show corresponding exothermic transitions at about 300 °C (Figure 15). Both could be explained by the presence of dimers which undergo cyclotrimerization at very high temperatures. The shallow transition of the liquid-crystalline samples are caused by a broad distribution of the end-to-end distance of cross-link sites. For all isotropic mixtures this distribution is narrower and leads to well-

(27) Gordon, M.; Taylor, J. S. *J. Appl. Chem.* **1952**, *2*, 493.
(28) Owusu, A. O.; Martin, G. C.; Gotro, J. T. *Polym. Eng. Sci.* **1991**, *31*, 1604.
(29) Simha, R. *Macromolecules* **1977**, *10*, 1025.
(30) Pascault, J. P.; Galy, J.; Mechin, F. *Chemistry and Technology of Cyanate Ester Resins*; Hammerton, I., Ed.; Chapman and Hall: New York, 1994; p 114.
(31) Grenier-Loustalot, M. F.; Lartigau, C.; Metras, F.; Grenier, P. *J. Polym. Sci., Polym. Chem. Ed.* **1996**, *34*, 2955.

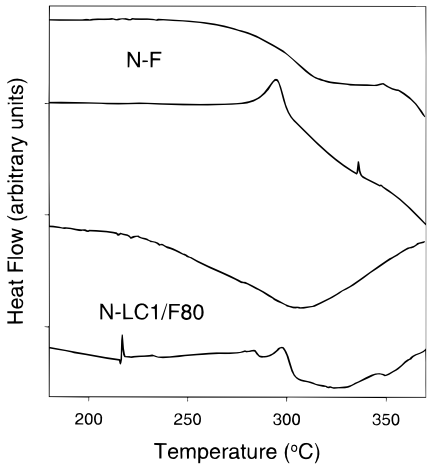

Figure 15. Temperature scans by DSC showing side reaction for thermoset mixtures LC1/F80 and pure F.

defined transitions. The LC field has a substantial influence on the curing. Domains in the LC phase may act as localized regions and determine the distribution of cross-link site distances, hence the macroscopic phase behavior.

Conclusions

The synthesis and physicochemical properties of several triazine networks prepared by a thermal cyclotrimerization reaction of mixtures between mesogenic dicyanates and commercial aromatic dicyanates are described. The various mixtures display liquid-crystalline behavior provided that a minimum of 50% of the mesogenic dicyanate is present, whereas in compositions containing less than 50% of the mesogenic dicyanate, the mixtures develop an isotropic phase. Accordingly, it is possible to obtain isotropic or nematic networks by appropriately adjusting the composition. DSC and FT/IR measurements allowed us to find the best conditions for the cyclotrimerization reaction and networks with reproducible properties were prepared and studied for their dynamic-mechanical behavior. A complex curing behavior with respect to the composition of the different mixtures could be shown by DSC measurements. These results emphasize that mixtures of LC dicyanates and non-LC dicyanates form a thermoset system in delicate balance. Although FT/IR measurements indicate that curing is complete, DSC and DMA measurements show contrary behavior in the resultant networks. The α-network relaxation temperature dependence from DMA measurements in the two systems shows a discrepancy from linear behavior. For both networks the α-network relaxation temperature is constant until monomer concentration is lower than 60% and then the α temperature decreases. The substantial deviations on the composition dependence by the network relaxation temperature from linear behavior, usually observed for binary systems, could be indicative of the presence of specific interactions between the dicyanate monomers LC1 and F or B. This may produce a reduction of the free volume and, consequently, an increase in the α-relaxation temperature value with respect to the one expected for noninteracting systems.

The wide variety of cyanate resin monomers available allows the tailoring of LC thermoset properties to a great extent. Blending different cyanate compounds is straightforward and may improve not only the rheological properties of the blend but also the properties of the cured resin. The introduction of an LC thermosetting monomer broadens this potential and almost any desired property, such as T_g, modulus, and moisture uptake can be obtained. A very important fact for mixtures with a LC component is that these materials can be aligned in external fields and mechanical and thermal properties can be controlled anisotropically.[18] In this fashion waveguides might be developed, based on mixtures of commercially available cyanate ester resins and cyanate-functionalized LC compounds. The permanently locked-in orientation of a LC dye would lead to materials with a higher refractive index, low loss, and higher T_g. When both monomers are used without precuring, this strategy can be used to construct a guest−host system, in which the liquid-crystalline compound induces anisotropy at a certain ratio of non-LC material. An orientation of the LC compound in an external field (magnetic or electrical field) would lead to a macroscopic alignment of the whole mixture.

Further experimental work appears necessary to elucidate the peculiar role of the inherent reactivity of the chemically different dicyanates on the morphological structure of the networks as well as to assess the nature of the interactions between the dicyanates. There are still many questions open concerning the chemistry and kinetics of the curing reaction of dicyanates, especially in a liquid-crystalline environment. Answers to some of these puzzles may lie in the occurrence of intramolecular as well as intermolecular trimerization and even dimerization is possible in minor amounts. We have shown that a binary mixture of a rigid-rod monomer and a semiflexible monomer may be one possible way to adjust the molecular packing and maximize performance in a rigid-rod network. Additional studies with model compounds need to be carried out to obtain a complete understanding of the curing of cyanates and LC cyanates.

Acknowledgment. Grants from IBM Systems Technology Division and the National Science Foundation, Division of Materials Research, are acknowledged. The authors would like to thank the Air Force Office of Sponsored Research and Japan Synthetic Rubber (JSR) for partial support of this work. Support by the Industry-Cornell Alliance for Electronic Packaging is also appreciated. H.K. would like to thank the Fulbright Commission for partial support. The use of the facilities at the Cornell Materials Science Center is acknowledged. We thank M. J. Valentine for extensive POM experiments. Finally, this work was partially supported by MURST and by the National Research Council of Italy (Progetto Chimica Fine 2—Sottoprogetto Materiali Polimerici).

CM960642E